Room-Temperature Assembly of Germanium Photonic Crystals through Colloidal Crystal Templating

Robert G. Shimmin,[†] Robert Vajtai,[‡] Richard W. Siegel,[‡,§] and Paul V. Braun*[,†]

Department of Materials Science and Engineering, Beckman Institute for Advanced Science and Technology, and Frederick Seitz Materials Research Laboratory, University of Illinois at Urbana−Champaign, 1304 W Green Street, Urbana, Illinois 61801, and Rensselaer Nanotechnology Center and Department of Materials Science and Engineering, Rensselaer Polytechnic Institute, 110 8th Street, Troy, New York 12180

Received December 7, 2006. Revised Manuscript Received February 12, 2007

Using an evaporation-driven, room-temperature infiltration technique, we filled the interstitial space within an opal formed from 1 μm polystyrene spheres with preformed germanium nanoparticles. Subsequently, the Ge nanoparticles were bound together by backfilling with a photocuring adhesive, and the original polystyrene template was etched away to yield an inverse opal of air spheres in a matrix of Ge nanoparticles and photoadhesive. The reflectance spectra of these photonic materials were compared to computed band structures to deduce the refractive index of the air−germanium and air−photoadhesive composites; in conjunction with the Maxwell-Garnett model of dielectric mixing, this comparison also allowed the estimation of the Ge volume fraction within each composite material. On the basis of these methods, the interstitial space of the initial polystyrene opal template was filled to 49 vol % with Ge nanoparticles, acquiring an effective refractive index of 1.74. Backfilling with photoadhesive, followed by removal of the polystyrene opal, produced a Ge-in-polymer composite with a refractive index contrast of 2.05.

Introduction

Inverse opals are materials containing three-dimensionally periodic arrays of air pores within a matrix of some functional material. This periodic structure leads to a periodic variation in refractive index that can result in strong optical diffraction, and face-centered cubic inverse opals with sufficient refractive index contrast (air pores in a matrix of $n \geq 2.9$) feature a complete photonic band gap.[1]

Many published methods for fabricating inverse opals begin by assembling an opal template from monodisperse silica or polystyrene spheres using vertical deposition,[2] sedimentation,[3] or flow cells.[4] A functional material is then synthesized within the interstitial spaces of the opal template, and the template is subsequently etched away. Routes for synthesizing a functional material within the pores of the template opal include electrodeposition,[5,6] chemical bath deposition,[7] sol−gel techniques,[8−10] chemical vapor deposition,[11,12] and atomic layer deposition.[13,14] These techniques, in which the functional material is synthesized within the opal template, require that the template retain its shape under the conditions of the functional material's synthesis.

In contrast, another approach, interesting in that it does not require the template material to be robust under the conditions of the functional material's synthesis, is the incorporation of preformed nanoparticles into an opaline template. This can be accomplished by decorating colloidal particles with nanoparticles prior to colloidal assembly, by co-assembling the nanoparticles with the colloids, or, as in the present work, infiltrating the nanoparticles into the already-assembled opal. Such approaches provide a means to incorporate fluorescent,[15,16] luminescent,[17−20] plasmonic,[21−24]

* Corresponding author. E-mail: pbraun@uiuc.edu. Phone: 217-244-7293. Fax: 217-333-2736.
[†] University of Illinois at Urbana−Champaign.
[‡] Rensselaer Nanotechnology Center, Rensselaer Polytechnic Institute.
[§] Department of Materials Science and Engieering, Rensselaer Polytechnic Institute.

(1) Busch, K.; John, S. *Phys. Rev. E* **1998**, *58*, 3896−3908.
(2) Jiang, P.; Bertone, J. F.; Hwang, K. S.; Colvin, V. L. *Chem. Mater.* **1999**, *11*, 2132−2140.
(3) Davis, K. E.; Russel, W. B.; Glantschnig, W. J. *Science* **1989**, *245*, 507−510.
(4) Park, S. H.; Qin, D.; Xia, Y. *Adv. Mater.* **1998**, *10*, 1028−1032.
(5) Xu, L.; Tung, L. D.; Spinu, L.; Zakhidov, A. A.; Baughman, R. H.; Wiley, J. B. *Adv. Mater.* **2003**, *15*, 1562−1564.
(6) Yeo, K. H.; Teh, L. K.; Wong, C. C. *J. Cryst. Growth* **2006**, *287*, 180−184.
(7) Blanco, A.; López, C.; Mayoral, R.; Míguez, H.; Meseguer, F.; Mifsud, A.; Herrero, J. *Appl. Phys. Lett.* **1998**, *73*, 1781−1783.
(8) Wijnhoven, J. E. G. J.; Bechger, L.; Vos, W. L. *Chem. Mater.* **2001**, *13*, 4486−4499.
(9) Scott, R. W. J.; Yang, S. M.; Chabanis, G.; Coombs, N.; Williams, D. E.; Ozin, G. A. *Adv. Mater.* **2001**, *13*, 1468−1472.
(10) Li, B.; Zhou, J.; Hao, L.; Hu, W.; Zong, R.; Cai, M.; Fu, M.; Gui, Z.; Li, L.; Li, Q. *Appl. Phys. A* **2003**, *82*, 3617−3619.
(11) Blanco, A.; Chomski, E.; Grabtchak, S.; Ibisate, M.; John, S.; Leonard, S. W.; Lopez, C.; Meseguer, F.; Miguez, H.; Mondia, J. P.; Ozin, G. A.; Toader, O.; van Driel, H. M. *Nature* **2000**, *405*, 437−440.
(12) Míguez, H.; Chomski, E.; García-Santamaría, F.; Ibisate, M.; John, S.; López, C.; Meseguer, F.; Mondia, J. P.; Ozin, G. A.; Toader, O.; Driel, H. M. v. *Adv. Mater.* **2001**, *13*, 1634−1637.
(13) King, J. S.; Graugnard, E.; Summers, C. J. *Adv. Mater.* **2005**, *17*, 1010−1013.
(14) Rugge, A.; Park, J. S.; Gordon, R. G.; Tolbert, S. H. *J. Phys. Chem. B.* **2005**, *109*, 3764−3771.
(15) Zhang, J.; Coombs, N.; Kumacheva, E. *J. Am. Chem. Soc.* **2002**, *124*, 14512−14513.
(16) Zhang, J.; Coombs, N.; Kumacheva, E.; Lin, Y.; Sargent, E. H. *Adv. Mater.* **2002**, *14*, 1756−1759.
(17) Lin, Y.; Zhang, J.; Sargent, E. H.; Kumacheva, E. *Appl. Phys. Lett.* **2002**, *81*, 3134−3136.

10.1021/cm062893l CCC: $37.00
Published on Web 03/21/2007

and otherwise optically interesting nanoparticles into a photonic crystal. When larger quantities of nanoparticles are introduced into the opal, the nanoparticles can fill the void space within the opal, and, usually after sintering the nanoparticles together, the colloidal template can be removed to yield a three-dimensionally ordered macroporous solid, or inverse opal. However, this sintering operation often leads to serious crack formation and other deformations. Inverse opals of oxides,[25−32] zeolites,[33] semiconductors,[34,35] metals,[36,37] and intermetallic compounds[38] have all been prepared from preformed nanoparticles templated by colloidal self-assembly.

In the present paper, we report the preparation of germanium-containing inverse opals by nanoparticle infiltration. Germanium has a very high refractive index ($n = 4.12$ at $\lambda = 2.0$ μm), making it of use in the fabrication of photonic band gap materials. Known methods of depositing germanium in a three-dimensionally ordered template, such as chemical vapor deposition[12] and hydrogen reduction of templated germanium oxide,[39] require temperatures greater than most polymeric materials can withstand. Yet many methods for fabricating three-dimensionally ordered templates, including self-assembly of latex microspheres,[2] holographic lithography,[40] phase-mask lithography,[41] and multiphoton photopolymerization,[42,43] have been most extensively developed for polymeric materials. We have deposited Ge nanoparticles in a polystyrene opal template and converted this structure into a Ge-containing inverse opal using only room-temperature processing techniques. Ge nanoparticles were infiltrated into a polystyrene opal and then fixed in place in a photocurable polymer matrix. Finally, the polystyrene template was dissolved in toluene. The resulting Ge-in-polymer composite has a refractive index of $n = 2.05$.

We also show here how the shift in the wavelength of peak reflectance that occurs when a photonic crystal is infiltrated with nanoparticles can be quantitatively related, through band structure calculations and the Maxwell-Garnett model of dielectric mixing,[44] to the volume fraction of the photonic crystal occupied by nanoparticles. This provides a facile, nondestructive means of measuring the nanoparticle content of an infiltrated photonic crystal, useful for judging the extent of infiltration whether the goal of a particular application is maximal infilling, or some specific nanoparticle content.

Experimental Section

Germanium Nanoparticle Synthesis. Ge nanoparticles were produced by the inert gas method.[45] Bulk germanium was loaded into a tungsten wire basket in a high-vacuum chamber, which was then evacuated to 1×10^{-4} Pa to clean deposited species from its surfaces. The chamber was then backfilled with an inert gas, typically with 40 Torr He. The germanium was evaporated by resistive heating into the high-purity gas atmosphere, where collisions with the gas atoms cool the evaporated germanium atoms, resulting in germanium cluster and nanoparticle formation. The nanoparticles became deposited by thermophoresis on a cold finger in the chamber, and after being cooled in vacuum, they were mechanically collected as a suspension in ethanol. The process requires convection in the inert gas atmosphere and results in a log-normal nanoparticle size distribution.[46]

The size distribution seen in the micrograph of Figure 1a, with most particles in the range 25−100 nm, is typical of the nanoparticles used in this work. Because the nanoparticles are to be used to infiltrate a synthetic opal, their size distribution should include few if any particles larger than the smallest pores within the opal; for the opals of face-centered cubic packed 1.0 μm spheres used in the present work, particles no larger than 150 nm could pass through the triangular pores within the opal. Despite the log-normal size distribution of the Ge nanoparticles prepared by the gas condensation method, transmission electron microscopy of the Ge nanoparticles used in this work found few particles larger than 120 nm. To gauge whether numerically rare large particles in the Ge suspension would impede its infiltration into packed 1.0 μm spheres, we compared opals infiltrated with the as-prepared Ge suspension (using the methods described below) with opals infiltrated with a Ge suspension from which the large end of the size distribution had been removed by centrifugation. Removing the largest particles from the Ge size distribution in this fashion did not increase the

(18) Rogach, A.; Susha, A.; Caruso, F.; Sukhorukov, G.; Kornowski, A.; Kershaw, S.; Möhwald, H.; Eychmüller, A.; Weller, H. *Adv. Mater.* **2000**, *12*, 333−337.
(19) Rogach, A. L.; Nagesha, D.; Ostrander, J. W.; Giersig, M.; Kotov, N. A. *Chem. Mater.* **2000**, *12*, 2676−2685.
(20) Wang, D.; Rogach, A. L.; Caruso, F. *Chem. Mater.* **2003**, *15*, 2274−2729.
(21) Chen, H.-H.; Suzuki, H.; Sato, O.; Gu, Z.-Z. *Appl. Phys. A* **2005**, *81*, 1127−1130.
(22) Liang, Z.; Susha, A. S.; Caruso, F. *Adv. Mater.* **2002**, *14*, 1160−1164.
(23) Liang, Z.; Susha, A.; Caruso, F. *Chem. Mater.* **2003**, *15*, 3176−3183.
(24) Romanov, S. G.; Susha, A. S.; Torres, C. M. S.; Liang, Z.; Caruso, F. *J. Appl. Phys.* **2005**, *97*, 086103.
(25) Gu, Z.-Z.; Kubo, S.; Qian, W.; Einaga, Y.; Tryk, D. A.; Fujishima, A.; Sato, O. *Langmuir* **2001**, *17*, 6751−6753.
(26) Gu, Z.-Z.; Kubo, S.; Fujishima, A.; Sato, O. *Appl. Phys. A* **2002**, *74*, 127−129.
(27) Iskandar, F.; Abdullah, M.; Yoden, H.; Okuyama, K. *J. Appl. Phys.* **2003**, *93*, 9237−9242.
(28) Iskandar, F.; Abdullah, M.; Yoden, H.; Okuyama, K. *J. Sol−Gel Sci. Technol.* **2004**, *29*, 41−47.
(29) Kuai, S.; Badilescu, S.; Bader, G.; Brüning, R.; Hu, X.; Truong, V. V. *Adv. Mater.* **2003**, *15*, 73−75.
(30) Kuai, S. L.; Hu, X. F.; Truong, V. V. *J. Cryst. Growth* **2003**, *259*, 404−410.
(31) Subramania, G.; Constant, K.; Biswas, R.; Sigalas, M. M.; Ho, K. M. *J. Lightwave Technol.* **1999**, *17*, 1970−1974.
(32) Subramania, G.; Constant, K.; Biswas, R.; Sigalas, M. M.; Ho, K.-M. *Adv. Mater.* **2001**, *13*, 443−446.
(33) Valtchev, V. *J. Mater. Chem.* **2002**, *12*, 1914−1918.
(34) Vlasov, Y. A.; Yao, N.; Norris, D. J. *Adv. Mater.* **1999**, *11*, 165−169.
(35) Yang, L.; Yang, Z.; Cao, W.; Chen, L.; Xu, J.; Zhang, H. *J. Phys. Chem. B* **2005**, *109*, 11501−11504.
(36) Velev, O. D.; Tessier, P. M.; Lenhoff, A. M.; Kaler, E. W. *Nature* **1999**, *401*, 548.
(37) Lu, L.; Capek, R.; Kornowski, A.; Gaponik, N.; Eychmüller, A. *Angew. Chem., Int. Ed.* **2005**, *44*, 5997−6001.
(38) Schaak, R. E.; Sra, A. K.; Leonard, B. M.; Cable, R. E.; Bauer, J. C.; Han, Y. F.; Means, J.; Teizer, W.; Vasquez, Y.; Funck, E. S. *J. Am. Chem. Soc.* **2005**, *127*.
(39) Míguez, H.; Meseguer, F.; López, C.; Holgado, M.; Andreasen, G.; Mifsud, A.; Fornés, V. *Langmuir* **2000**, *16*, 4405−4408.
(40) Campbell, M.; Sharp, D. N.; Harrison, M. T.; Denning, R. G.; Turberfield, A. J. *Nature* **2000**, *404*, 53−56.
(41) Jeon, S.; Park, J. U.; Cirelli, R.; Yang, S.; Heitzman, C. E.; Braun, P. V.; Kenis, P. J. A.; Rogers, J. A. *Proc. Natl. Acad. Sci.* **2004**, *101*, 12428−12433.
(42) Straub, M.; Gu, M. *Opt. Lett.* **2002**, *27*, 1824−1826.
(43) Pruzinsky, S. A.; Braun, P. V. *Adv. Funct. Mater.* **2005**, *15*, 1995−2004.
(44) Maxwell-Garnett, J. C. *Philos. Trans. R. Soc. London, Ser. A* **1904**, *203*, 385−420.
(45) Siegel, R. W. *Annu. Rev. Mater. Sci.* **1991**, *21*, 559−578.
(46) Söderlund, J.; Kiss, L. B.; Niklasson, G. A.; Granqvist, C. G. *Phys. Rev. Lett.* **1998**, *80*, 2386−2388.

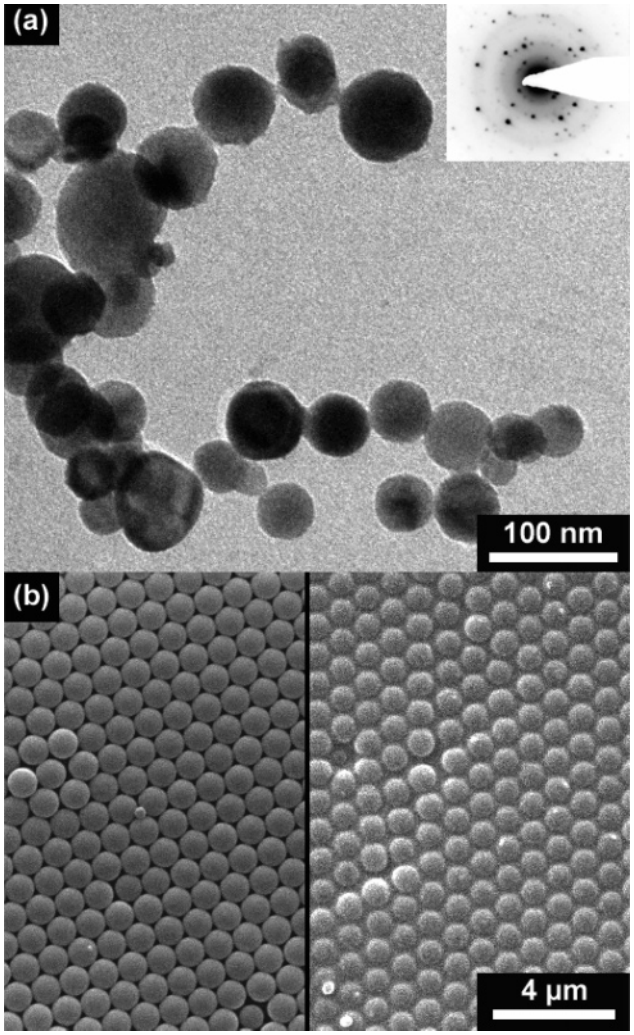

Figure 1. (a) TEM of germanium nanoparticles. Inset: selected area electron diffraction pattern from these nanoparticles. (b) Top view of vertically deposited polystyrene opal, (left) as deposited and (right) after infiltration with Ge nanoparticles.

volume fraction of Ge in the infiltrated opal. The Ge-containing opal structures discussed in the remainder of the present work were prepared using the Ge nanoparticle suspension as initially prepared.

Polystyrene Opal Assembly. Polystyrene opals were prepared by vertical deposition.[2] Sulfate polystyrene microspheres, diameter 1.0 μm, were purchased from the Interfacial Dynamics Corporation (batch no. 2293,1; CV 4.2%). These were diluted to 0.4% by volume with deionized water, and 6 mL of the dilute colloidal suspension was placed in a low-density polyethylene vial, internal diameter 22 mm, total capacity 12 mL (Nalge Nunc International). A glass substrate, 17 mm wide, was cut from a microscope slide (Corning 2947), cleaned by immersing it for 5 min in 5% aqueous HF (***caution:*** *HF is highly toxic. Both skin contact and inhalation of its fumes must be strictly prevented*), thoroughly rinsed in deionized water, wicked dry by placing its bottom edge against a Kim-wipe, and then placed vertically in the colloidal suspension, as close to the vial perimeter as its width would permit. The colloidal suspension was maintained at 45 °C in a temperature-controlled aluminum-block dry bath (Fisher Scientific) until it evaporated to dryness, about 22 h. Following deposition, the opals were sintered for 1 h at 80 °C.

Opal Inversion with Ge/NOA-63 Composite. Figure 2 illustrates the apparatus used for the evaporation-driven infiltration of Ge nanoparticles into polystyrene opals. A shallow plastic vial (depth 9 mm, total capacity 3.8 mL) was nearly filled with the

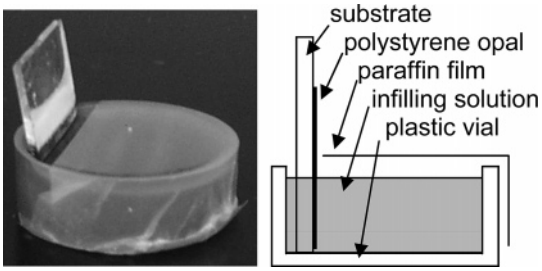

Figure 2. Photograph and schematic of the apparatus used for evaporation-driven backfilling of synthetic opals.

solution of Ge nanoparticles in ethanol. The vial was mostly covered with paraffin film, leaving open a segment just large enough to admit the opal and its substrate; the purpose of this covering was to maintain an elevated partial pressure of ethanol within the vial, and in so doing, to enhance the fraction of the evaporative flux of ethanol passing through the wet opal, which protruded above this covering. A sintered polystyrene opal was then set vertically in the nanoparticle solution, through this opening, and the solution was allowed to evaporate to dryness. As the solution dries, Ge nanoparticles infiltrate the opal, filling a band across the opal marking the highest ascent of solvent wicked up into the opal. Figure 1b shows the top surface of this Ge-filled region, illustrating the effective filling of the opal's void space with nanoparticles.

To backfill the nanoparticle-filled opal with Norland Optical Adhesive 63 (NOA-63), a UV-curing photoadhesive, we repeated the procedure used for nanoparticle infiltration, using a 1.5 wt % solution of NOA-63 in ethanol in place of the nanoparticle solution. The optical adhesive was then cured by illumination under a 100 W longwave UV lamp for 1 h. To complete the inversion, we etched the polystyrene in toluene for 8 h. Although the Ge-containing regions of inverse opals did not delaminate from the substrate during etching, other regions often did. The Ge-containing samples were rinsed by being immersed for 5 min successively in fresh toluene, a solution of equal volumes toluene and ethanol, and then ethanol, before being dried from ethanol using supercritical carbon dioxide.

Opal Inversion with NOA-63. A drop of NOA-63 was deposited on the sintered polystyrene opal. The adhesive was spread into the opal by clamping it between the opal substrate and a glass cover slip, previously rendered hydrophobic by immersion in a hexane solution of octadecyltrichlorosilane. As the adhesive penetrated the opal, the opal became translucent while remaining opalescent. The optical adhesive was then cured by illumination beneath a 100 W longwave UV lamp for 1 h.

To complete the inversion, we removed the cover slip and etched the polystyrene for 8 h in toluene. During this etch, the NOA film delaminated from the substrate, becoming a free-floating inverse opal film. This film was gradually "deswelled" by withdrawing solvent from the etch solution and replacing it with ethanol until the entire volume of the solvent bath had been exchanged twice over. The inverse opal film was then recovered by mechanically positioning it flat on a glass slide as it was dried from ethanol.[47] The inverse opal was positioned with its original top face against the new substrate, to make the original bottom face viewable by SEM.

Infrared Spectroscopy. Infrared reflectance spectroscopy was performed through an infrared microscope (Bruker Hyperion) coupled to an FTIR spectrometer (Bruker Vertex 70), using a tungsten filament infrared light source, CaF_2 beamsplitter, and InSb detector, optical components appropriate to the wavelength range of interest (0.9−3.3 μm). The beam was focused onto the sample

(47) Mach, P.; Wiltzius, P.; Megens, M.; Weitz, D. A.; Lin, K. h.; Lubensky, T. C.; Yodh, A. G. *Europhys. Lett.* **2002**, *58*, 679−685.

at normal incidence through a 4× glass objective with a numerical aperture (NA)[48] of 0.10. A physical aperture limited the spot size to 200 μm, so that spectra were taken from small, spatially resolved regions of the opal.[49] All reflectance spectra were normalized against that from an aluminum mirror.

Results and Discussion

The dielectric function ϵ_c of a composite material consisting of infinitely small particles embedded in a matrix may be calculated from the dielectric functions of the matrix (ϵ_m) and the particles (ϵ_p) by the Maxwell-Garnett model

$$\frac{\epsilon_c - \epsilon_m}{\epsilon_c + \kappa\epsilon_m} = f_p \frac{\epsilon_p - \epsilon_m}{\epsilon_p + \kappa\epsilon_m} \quad (1)$$

where f_p is the volume fraction of the particles in the composite and κ is a screening parameter dependent on particle shape. For infinitely small spheres, $\kappa = 2$. The Maxwell-Garnett model can be extended to particles of finite size by the dynamic Maxwell-Garnett model,[50,51] in which κ is replaced by a dynamic, wavelength-dependent screening function. For 50 nm spheres illuminated by light of 1.5−3 μm wavelength, accounting for finite-size effects alters the index of refraction predicted for the composite material by 1% or less.

The wavelength of peak reflectance from a face-centered cubic opal depends on the direction of illumination and the refractive indices of the opal spheres and opal matrix material and can be computed using plane-wave expansion (PWE) band structure calculations.[52] For modeling the wavelength of the IR reflectance peak, it is not necessary to compute the complete band structure, but merely the dispersion relationship in the Γ−L (<111>) direction. For an opal containing spheres of known refractive index in a matrix of unknown refractive index, the unknown matrix refractive index can be deduced by comparing the experimental reflectance spectrum of the opal to the computed peak positions calculated for a range of matrix refractive indices. This method allows one to determine the matrix refractive index, and coupled with eq 1, the nanoparticle volume fraction, of the air−nanoparticle composite that comprises the matrix of a nanoparticle-infiltrated opal.

Figure 3a compares the measured normal-incidence reflectance spectrum of a synthetic opal prepared from 1 μm diameter polystyrene microspheres, to the measured reflectance spectrum of that same opal, infiltrated with germanium nanoparticles. The spacing of the Fabry−Perot fringes in the reflectance spectrum of the initial polystyrene opal implies an opal 21 layers thick, thick enough that errors resulting from comparing the reflectance spectrum of this finitely thick opal to PWE calculations for an infinitely thick opal are small.[53]

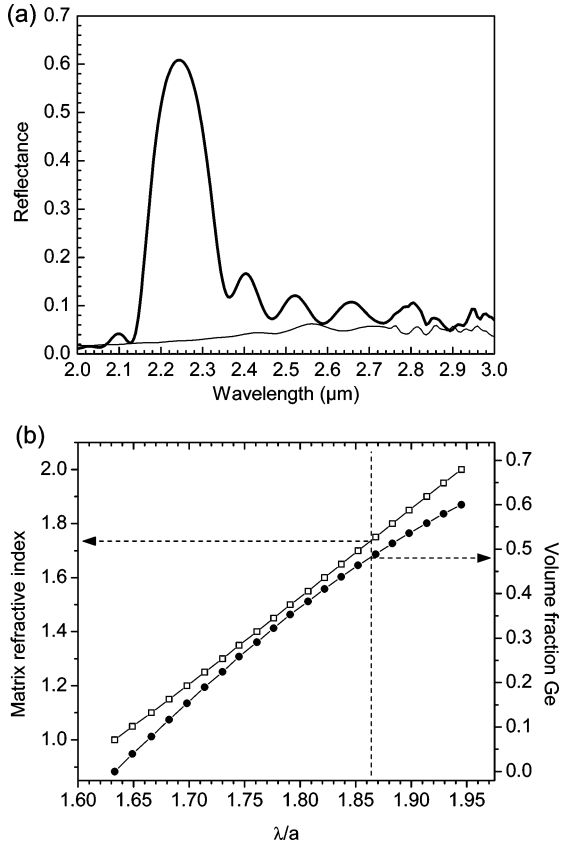

Figure 3. (a) Normal-incidence reflectance spectra of polystyrene opals, as grown (thick line) and infiltrated with Ge nanoparticles (thin line). (b) Refractive index (open squares) and Ge volume fraction (filled circles) of an air−germanium composite filling the interstitial spaces of a face-centered cubic polystyrene ($n = 1.57$) opal, as a function of the peak reflectance wavelength of the filled opal for normal incidence in the <111> direction. Wavelength is normalized against the fcc unit-cell length of 1.41 μm. The dependence of peak reflectance wavelength on matrix refractive index is computed using PWE band structure calculations, whereas the relationship between refractive index and germanium content comes from the Maxwell-Garnett model. Dotted lines indicate the matrix refractive index and Ge volume fraction for the Ge-infiltrated opal whose reflectance spectrum is shown in Figure 3a.

Infiltration with Ge nanoparticles shifts the reflectance peak from 2.24 to 2.56 μm, while sharply reducing reflected intensity. According to Figure 3b, this 14% shift in peak reflectance corresponds to a change in the matrix from air ($n = 1$) to an air−germanium composite with $n = 1.74$, and thus a germanium volume fraction of 49%. The drop in reflected intensity can be attributed to the air−germanium composite more nearly matching the refractive index of polystyrene ($n = 1.57$) than air. To the eye, the Ge-filled portion of the opal appears dark in reflection, but translucent to transmitted light.

To prepare an inverse opal with greater refractive index contrast, the Ge-infiltrated opal was backfilled with NOA-63, and after curing the photoadhesive, the polystyrene spheres were etched away in toluene. The resulting inverse opal contained air spheres in a Ge−NOA composite matrix. The process of backfilling with NOA-63 results in an overlayer covering the Ge-infiltrated portion of the opal; this layer does not form over that portion of the opal not filled

(48) Lee, Y. J.; Pruzinsky, S. A.; Braun, P. V. *Opt. Lett.* **2005**, *30*, 153−155.
(49) Vlasov, Y. A.; Deutsch, M.; Norris, D. J. *Appl. Phys. Lett.* **2000**, *76*, 1627−1629.
(50) Foss, C. A.; Hornyak, G. L.; Stockert, J. A.; Martin, C. R. *J. Phys. Chem.* **1994**, *98*, 2963−2971.
(51) Hornyak, G. L.; Patrissi, C. J.; Martin, C. R. *J. Phys. Chem. B* **1997**, *101*, 1548−1555.
(52) Steven Johnson, J. J. *Opt. Express* **2001**, *8*, 173−190.
(53) Galisteo-López, J. F.; Palacios-Lidón, E.; Castillo-Martínez, E.; López, C. *Phys. Rev. B* **2003**, *68*, 115109.

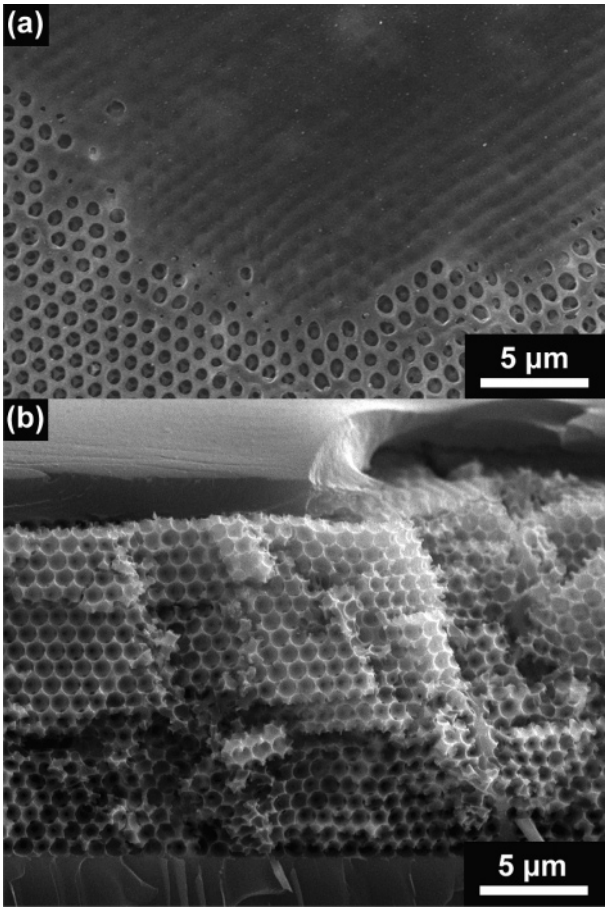

Figure 4. (a) A polymer layer selectively covers the Ge-containing region of the NOA-63 inverse opal. (b) SEM cross-section of the Ge-NOA composite inverse opal. The glass substrate is at the bottom of the image.

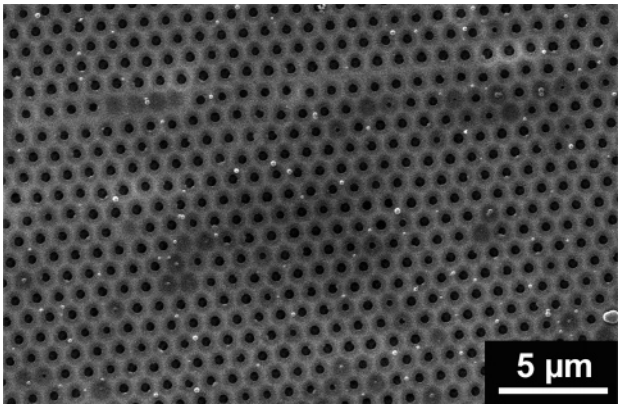

Figure 5. Top view of an NOA-63 inverse opal, prepared without germanium.

with Ge nanoparticles (Figure 4a). The germanium−NOA composite inverse opal beneath this overlayer can be plainly seen in cross-sectional SEM (Figure 4b).

To serve as a reference with which to compare the Ge-NOA composite inverse opal system, inverse opals were also prepared using NOA-63 alone, without germanium nanoparticles. Although microscopy of these inverse opals' upper surfaces (Figure 5) shows that the 1.0 μm spacing of the polystyrene template spheres is preserved in the spacing of the air spheres in the inverse opal, the IR reflectance spectrum of such inverse opals (Figure 6a), with peak reflectance at 1.61 μm, is not consistent with an inverse opal

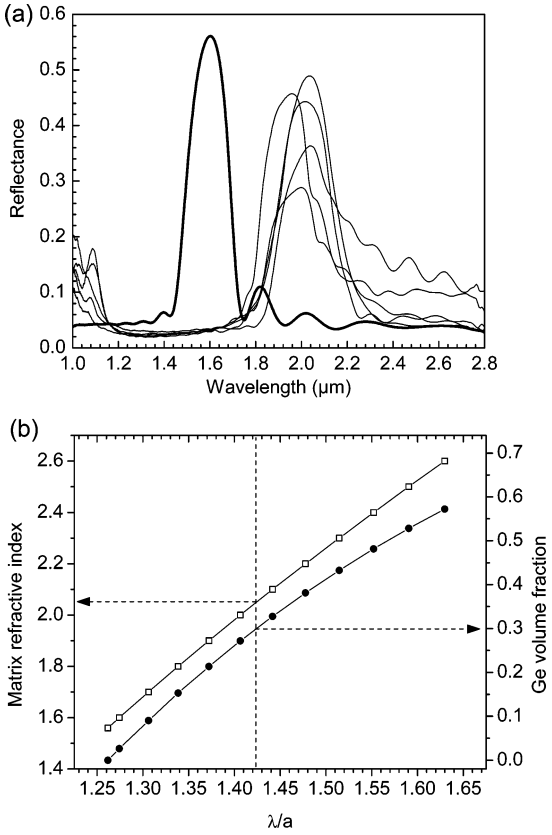

Figure 6. (a) Normal-incidence reflectance spectra of NOA-63 inverse opals templated from vertically deposited polystyrene opals, containing Ge nanoparticles (thin lines), compared to a Ge-free reference sample (thick line). (b) Refractive index (open squares) and Ge volume fraction (filled circles) of a germanium−NOA composite filling the space between oblate air spheroids with aspect ratio 0.95, packed on a face-centered cubic lattice distorted by 5% compression in the <111> direction. Wavelength is normalized against the (uncompressed) fcc unit-cell length of 1.41 μm. Dotted lines indicate the refractive index and Ge content for a Ge-containing inverse opal with peak reflectance at 2.01 μm, the mean peak position of the five spectra from Ge-containing inverse opals shown in Figure 6a.

of 1.0 μm air spheres in an NOA-63 matrix ($n = 1.56$). Rather, the position of this reflectance peak is consistent with an inverse opal of oblate air spheroids in NOA-63, where the aspect ratio of the air spheroids is 0.85. In the process of being dried on a substrate, the inverse opal shrinks, but only in the direction normal to the substrate.[54]

The Ge−NOA composite inverse opal shows less shrinkage in the normal direction. Viewed from the top (Figure 4a), the air pores have the 1.0 μm spacing of the polystyrene template, whereas the cross-sectional micrograph of Figure 4b shows 21 layers of air pores, and the measured thickness from the center of the top layer to the center of the bottom layer is 95% of that expected of a packing of spheres. Evidence that this small degree of shrinkage is consistent throughout the Ge-filled region comes from the spectra of Figure 6a. Here, the peak reflectance wavelengths of several spectra taken from locations throughout the Ge-filled part of a Ge−NOA composite inverse opal span the range 1.96−2.04 μm, a degree of consistency suggesting some degree of uniformity in both layer spacing and refractive index

(54) Lee, Y. J.; Pruzinsky, S. A.; Braun, P. V. *Langmuir* **2004**, *20*, 3096−3106.

across the Ge-filled portion of the inverse opal. The mean peak reflectance wavelength of these five spectra is 2.01 μm.

From PWE band structure calculations, a face-centered cubic inverse opal of close-packed 1.0 μm air spheres in an NOA-63 ($n = 1.56$) matrix, distorted by 5% compression in the <111> direction, so that the inverse opal becomes a packing of aspect ratio 0.95 oblate air spheroids in an $n = 1.56$ matrix, has peak reflectance at 1.78 μm for normal-incidence reflection in the <111> direction. According to Figure 6b, the 13% shift in peak wavelength between this calculated spectrum and the measured spectra of Ge-NOA composite inverse opals implies that the Ge-in-NOA matrix of these inverse opals has $n = 2.05$ and 30% Ge volume fraction.

The 30% Ge volume fraction derived for the Ge-in-NOA composite is less than the 49% Ge volume fraction derived for the Ge-in-air composite from which it was formed. One hypothesis is that the Ge-in-NOA composite actually has a higher Ge volume fraction, but NOA does not fill all the space between the germanium nanoparticles, and the remaining air, not included in the model of Figure 6b, results in a lower refractive index for any given Ge volume fraction: a composite containing, by volume, 49% Ge nanoparticles in 18% NOA and 33% air would have the same refractive index (2.05) as one containing 30% Ge nanoparticles and 70% NOA. Another hypothesis lies in the observation that these NOA-63 inverse opals feature an overlayer only over that part of them that was filled with germanium nanoparticles: it is possible that the NOA-63 backfilling process expels some of the Ge nanoparticles into this overlayer. A complementary method for quantitatively determining the Ge content or nanometer-scale porosity of these structures would be useful.

It is worth noting that despite significant Ge volume fractions, the Ge−air and Ge−NOA composites fabricated for this work have refractive indices far short of germanium's. This is due to the Ge nanoparticles' existence as discrete particles within a continuous lower-index matrix: under these conditions, the composite refractive index depends more upon the refractive index of the matrix than upon that of the particles. If the Ge particles could be fully sintered together in a postprocessing step, or the use of faceted rather than rounded Ge nanoparticles could create significantly greater interparticle contacts, then a mean field approximation would describe the composite's refractive index better than the Maxwell-Garnett model and a given volume fraction of Ge would yield a higher refractive index for the composite. Still, the present refractive index contrast of 2.05 exceeds any other examples of which we are aware for a photonic crystal of discrete nanoparticles.

Conclusions

Using an evaporation-driven infiltration technique, we have filled polystyrene synthetic opals with germanium nanoparticles. The Maxwell-Garnett model of dielectric mixing provides a means to relate the reflectance spectrum of a filled opal to the degree of nanoparticle infiltration; using this method, we have calculated that we have filled up to 49% of the insterstitial volume of the polystyrene template with Ge nanoparticles, essentially filling the opal with a Ge−air composite of refractive index 1.74. The refractive index of this composite can be increased, and the Ge nanoparticles fixed in place, by backfilling with a photocuring adhesive. After etching away the polystyrene template, an inverse opal of air pores in a Ge−polymer matrix remains. The refractive index of this Ge−polymer composite is 2.05. Further gains in refractive index might be achievable through causing the Ge nanoparticles embedded in the composite to form a more continuous phase.

Acknowledgment. This work was supported by the Nanoscale Science and Engineering Initiative of the NSF under Award DMR-0117792. Research for this publication was carried out in part in the Center for Microanalysis of Materials, University of Illinois at Urbana−Champaign, which is partially supported by the U.S. Department of Energy under Grant DEFG02-91-ER45439. R.G.S. acknowledges fellowship support from the Fannie and John Hertz Foundation.

CM062893L